Optimal Capacity Estimation and Allocation of Distributed Generation Units with Suitable Placement of Electric Vehicle Charging Stations

Pavitra Sharma[1], Akhilesh Kumar Mishra[2], Puneet Mishra[3], Hitesh Dutt Mathur[4]
Department of Electrical & Electronics Engineering
Birla Institute of Technology & Science, Pilani
Pilani (Rajasthan), India
p20190027@pilani.bits-pilani.ac.in[1], p20170426@pilani.bits-pilani.ac.in[2], puneet.mishra@pilani.bits-pilani.ac.in[3], mathurhd@pilani.bits-pilani.ac.in[4]

2021 IEEE Region 10 Symposium (TENSYMP) | 978-1-6654-0026-8/21/$31.00 ©2021 IEEE | DOI: 10.1109/TENSYMP52854.2021.9550958

***Abstract*—The optimal capacity estimation and allocations of Distributed Generation (DG) units along with appropriate placement of Electric Vehicle charging stations (EVCS) makes a substantial contribution in curtailing power losses and improving the voltage stability of a system. In this regard, this paper formulates a multi-objective function to minimize the power losses and voltage deviation of buses in the distribution network. The optimization problem is solved using three different types of optimization algorithms, namely Particle Swarm Optimization (PSO), Grey Wolf Optimization (GWO), and Hybrid Particle Swarm Grey Wolf Optimization (HPSOGWO). To simulate the practical situation, voltage-dependent load and various electric vehicle (EV) charging patterns based on the location of EVCS are considered in this study. Solar photovoltaic, wind turbine, and diesel generator-based DGs are taken into account in this study. The proposed algorithm is tested on an IEEE 33 bus network considering different scenarios. The results obtained show that HPSOGWO provides the most optimal solution among all the considered algorithms, with the least power loss and voltage deviation for all scenarios.**

***Keywords*—Optimal allocation, Capacity estimation, Electric Vehicle charging stations, Distributed Generation, Hybrid Particle Swarm Grey Wolf Optimization**

I. INTRODUCTION

The small-scale power generation systems, connected close to consumer loads are known as Distributed Generation unit (DG). In recent years, the integration of DGs to the conventional grid has increased rapidly due to its advantages in technical, environmental, and economic aspects. Photovoltaic, Wind turbines, biomass, microturbines, fuel cells are the distributed energy resources that come under Distributed Generation. It is mentioned in [1], that in the upcoming days DG would contribute around 20% of total power generation. Along with DG, electric vehicles (EVs) are also getting popular as a potential alternative to fossil-fuel-driven transportation. The penetration of EVs in the network increases the system's total load which is a challenge for the current distribution system [2]. It is observed that power loss and voltage stability of an electrical network is dependent on DG's sizing, EVs charging load, location of DGs, and EVs charging stations (EVCS) in a network. Therefore, if the sizing of DGs and their integration with EVCS are planned optimally and strategically in a network then they are always committed to reduce the network's power losses, enhancement of voltage stability margin, improvement of voltage profile, improvement of power quality of supplied power and system reliability [3].

In the past few years, many algorithms have been formulated for optimal placement and capacity of DG for minimizing overall power losses in the distribution network [4][5][6][7][8]. In [4] the authors proposed an analytical technique to calculate the optimal location and size of Distributed Energy Resources (DERs). In [5] authors utilize an artificial bee colony algorithm to estimate the optimum location, power factor, and size of a DG unit. The study in [6] was focused on optimal allocation and sitting of photovoltaic PV cells in radial distribution systems based on the Ant Lion optimizer algorithm. The multi-objective function is formulated for the optimization problem but the authors did not present any information regarding the efficiency of the algorithm compared with other optimization algorithms. In [7] optimal allocation of DG units is done using a hybrid particle swarm optimization algorithm (HPSO). To place DG at a suitable position, loss sensitivity analysis is performed and for optimum sizing HPSO algorithm is used and results obtained are compared with other optimization algorithms. The work in [8] applied a hybrid method based on loss sensitivity factors and Moth-Flame optimization to determine the optimal placement and size of DG units. The loss sensitivity factors are used to estimate the candidate bus for DG allocation and Moth-Flame optimization is used to determine optimal size and placement of solar and wind-based DG units. Further, the authors of [9] aim to cut-down the total investment value by optimal placement of wind-based DG and battery storage system (BESS). The cost of investment for BESS and DG is taken to be proportional to their size. It is reported in [10], Hybrid Grey Wolf Optimization (HGWO) is suitable to solve the discrete, non-convex problems. Also, there is considerable reduction in loss and improvement in voltage profile. The results are compared with various metaheuristic algorithms and shows that the HGWO algorithm outshines all the other algorithms. The authors in [11] utilize grasshopper optimization (GOA) technique to determine the optimal place and size of DG units. The multi-objective function is formulated to minimize the active power losses and to improve voltage profile of the system. The voltage dependent electric load demand, and seasonal variations of wind and solar based DGs are considered but didn't take into account impact of electric vehicle charging load demand and optimal placement of electric vehicle charging stations. A genetic algorithm-based optimization problem is formulated in [12] to determine the optimal site and size of electric vehicle parking lots. The optimization problem considers the distribution system's reliability and power losses along with investment cost. However, this article didn't consider the renewable DG units and various electric vehicle charging patterns based on location of parking lots in the system. Further, an approach for simultaneous optimal allocation of renewable energy sources and EVCS in smart grids is proposed in [13]. A multi-objective optimization problem is formulated to reduce power losses, charging and demand supplying costs, and

voltage fluctuations. A hybrid genetic algorithm and particle swarm optimization are used to solve this multi-objective optimization problem but authors didn't discuss the impact of different electric vehicle charging patterns.

By the conducted literature survey, we remark that the researchers did not focus on optimal capacity estimation and allocations of DG units together with appropriate placement of EVCS simultaneously, and considering different charging patterns and voltage-dependent load. To investigate these issues, this paper formulates a multi-objective function with a purpose to determine the optimal capacity and location of multiple DGs along with EVCS, to reduce power losses and voltage fluctuations in the system. The considered test system includes voltage-dependent load models, renewable energy-based DG units, and different electric vehicle charging patterns.

The paper is organized as follows. Section II discusses the distributed generation units and load modelling. Electric vehicle charging load modelling is detailed in Section III. The objective function and operational constraints are formulated in Section IV. The results for the considered case study are presented in Section V. Lastly, Section VI concludes the paper.

II. Distributed Generation Units and Load Modelling

The DG units are usually modeled as a constant power factor model. Power electronic and synchronous generator-based DGs are referred to as controllable DGs [14]. In this study, all DGs are modelled as constant power factor model having a power factor of 0.9 lagging. The details of modelling of various DG units and electric load are discussed below.

A. Solar Photovoltaic (PV) as DG

The power output of a photovoltaic array is a function of solar insolation and its relation is shown in (1) [15].

$$Ppvg = \frac{G}{G_{STC}} * P_{rated}^{pvg} * \eta_{DC-DC}^{pvg} \quad (1)$$

where G stands for perpendicular irradiance falling on the PV array surface in W/m^2, η_{DC-DC}^{pvg} represents the converter efficiency of PV arrays which is assumed to be 95%. Moreover, P_{rated}^{pvg} is the rated value of the power of each PV array and G_{STC} is the solar irradiance at standard test condition (STC), which are considered to be 5 kW and 1000 W/m^2 respectively.

B. Wind turbine Generator (WTG) as DG

The power output of a wind turbine generator (WTG) is a function of wind speed and is expressed by (2) [15].

$$P_{WTG} = \begin{cases} 0\,; \quad v_w \le v_{ci,}, v_w \ge v_{co,} \\ P_{rated}^{WTG} * \left(\frac{v_w - v_{ci}}{v_r - v_{ci}}\right)^3 ;\ v_{ci} < v_w \le v_r \\ P_{rated}^{WTG} + \left(\frac{P_{co}^{WTG} - P_{rated}^{WTG}}{v_{co} - v_r}\right) * (v_w - v_r);\ v_r < v_w < v_{co} \end{cases} \quad (2)$$

where P_{WTG} is the active power output of WTG. Also, P_{co}^{WTG} and P_{rated}^{WTG} represents the active power output of WTG at cut-out and rated wind speed respectively. Furthermore, v_w, v_r, v_{ci} and v_{co} are measured, rated, cut-in, and cut-out wind speeds in m/sec respectively. The specifications of the considered WTG, including rated, cut-in, and cut-out wind speeds are 12.5 m/sec, 3.5 m/sec, 25 m/sec respectively. The WTG (Bonus 150/30) having a specified rated power of 150 kW is considered in this study [16].

C. Diesel Generator (DEG) as DG

The diesel generator having a constant power factor of 0.9 lagging is considered in this paper.

D. Electric Load Modelling

In a practical distribution system, the load is continuously changing. Therefore, this study considers voltage-dependent load i.e., residential, commercial, and industrial load models to simulate the practical scenario. In load flow problems, the here considered exponential-based static load modeling is more appropriate with respect to dynamic load modeling [17]. In the static load model, load behavior is represented as an algebraic function of voltage magnitude [17]. In the case of exponential load, the mathematical relation between the load parameters and voltage magnitude is shown in (3) & (4) [18].

$$P_{Load\,i} = P_{L0} V_i^{n_p} \quad i = 1,2,\ldots..N_b \quad (3)$$

$$Q_{Load\,i} = Q_{L0} V_i^{n_q} \quad i = 1,2,\ldots..N_b \quad (4)$$

where, n_p and n_q are active and reactive power exponents which vary according to different load classes i.e., residential, commercial, and industrial respectively. $P_{Load\,i}$ and $Q_{Load\,i}$ refers to real and reactive power load at i^{th} bus, while P_{L0} and Q_{L0} are the values of active and reactive power load at initial working conditions, respectively. V_i is the magnitude of the voltage at the i^{th} load bus. Table I shows the exponent values corresponding to different load types. In this paper, a winter day is considered and load type on buses is mentioned in Table II.

III. Electric Vehicle Charging Load Modelling

The stochastic behavior of EVs charging load is a result of several factors, such as the number of vehicles, battery capacity, time at which it is plugged in or plugged out, charging speeds, charging patterns, and daily distance traveled by an EV [19]. Moreover, various types of vehicles like private, public, buses behave differently which increases uncertainty in EV charging load. In this paper, EVs charging load is modelled using few parameters such as the number of vehicles, daily distance traveled by an EV, time at which it is plugged in i.e., arrival time or plugged out, i.e., departure time. The Monte Carlo simulation technique is used to estimate parameters such as daily distance, arrival, and departure time of EVs from their respective probability density functions.

It is assumed that EVs considered in this study are private vehicles. It is also assumed; the charging of EVs will start as soon as they reach their residence/workplace until the battery is fully charged. These EVs are charged according to the behaviors of three different charging station/parking nodes i.e., residential (RCS), commercial (CCS), and industrial (ICS) charging stations. At RCS, the EV charging starts at 4:00 pm after the owner arrives at the residence, whereas, for CCS it begins at 8:00 am when the owner arrives at the workplace. Usually, industrial employees have three kinds of working shifts therefore for ICS, at morning 6:00 am first shift's EV charging starts, similarly, the second shift and the third shift start at 2:00 pm and 10:00 pm respectively. The

duration of charging ($T_{C,n}$) for each n^{th} EV can be obtained from (5)[20].

$$T_{C,n} = \frac{D_n\, W_{100}^{EV}}{100\, P_{C,n}^{EV}\, \eta_C^{EV}} \quad \forall n \in N_e \tag{5}$$

where W_{100}^{EV} refers to the energy consumption per hundred kilometers in $kWh/100\ km$; P_C^{EV} represents the charging rate of EVs in kW; η_C^{EV} is the charging efficiency of EVs. N_e represents the total no. of EVs. The departure/end time ($T_{end,n}$) of EVs can be further calculated using (6) [20].

$$T_{end,n} = T_{start,n} + T_{c,n} - 1 \quad \forall n \in N_e \tag{6}$$

where $T_{start,n}$ represents the time at which EV charging begins. However, by accumulating the charging power of each period, the total charging load $P_{Load}^{EVs}(t)$ can be calculated. It is noted that EV charging periods are independent of each other, therefore, using (7) the daily load profile of a large number of EV charging can be calculated.

$$P_{Load}^{EVs}(t) = \sum_{n=1}^{N_e} P_{C,n}^{EV}(t) \tag{7}$$

where $P_{C,n}^{EV}$ is the charging power of n^{th} vehicle.

Figure 1 shows the daily charging load profile of 65 EVs at residential (RCS), commercial (CCS), and industrial (ICS) charging stations. Table III shows the parameters of electric vehicles considered in this work. The peak load of each EV charging load pattern is considered for determining optimal locations of four EVCS.

TABLE I. THE EXPONENT VALUES CORRESPONDING TO DIFFERENT LOAD TYPES[18]

Load Type		Residential		Commercial		Industrial	
		n_{pr}	n_{qr}	n_{pc}	n_{qc}	n_{pi}	n_{qi}
Summer	Day	0.72	2.96	1.25	3.5	0.18	0.6
	Night	0.92	4.04	0.99	3.95	0.18	0.6
Winter	Day	1.04	4.19	1.5	3.15	0.18	0.6
	Night	1.3	4.38	1.51	3.4	0.18	0.6
Constant Power		0	0	0	0	0	0

TABLE II. DIFFERENT LOAD TYPES ON VARIOUS BUSES

Load Type	Bus No.
Constant Power	2,3,4,5,6,7
Residential Load	8,9,10,11,12,13,14,15,16,17,18,19,20,21,22
Industrial Load	23,24,25
Commercial Load	26,27,28,29,30,31,32,33

TABLE III. PARAMETERS OF EV

PHEV Parameters	Value
W_{100}^{EV} (kWh/100km)	12
C_n^{EV} (kWh)	24
SOC_n^{max}/SOC_n^{min} (%)	100/20
$P_{C,n}^{EV}/P_{D,n}^{EV,max}$ (kW)	3
η_C^{EV}	85%

IV. OBJECTIVE FUNCTION FORMULATION AND OPERATIONAL CONSTRAINTS

In order to formulate the objective function, power flow calculation is an initial step. Conventional power flow algorithms such as Gauss-Seidel, Newton Raphson are incompetent for distribution network as it has low X/R ratio.

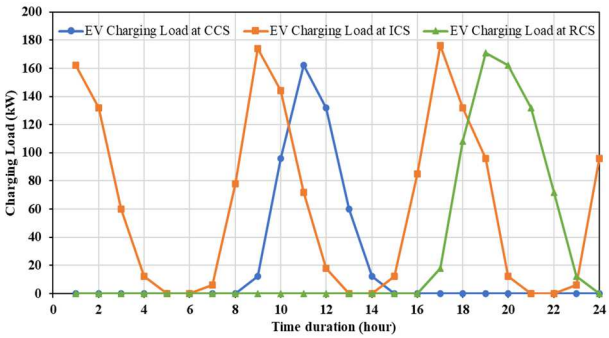

Fig. 1 Charging load profile of 65 number of EVs at residential (RCS), commercial (CCS) and industrial (ICS) charging station

Hence, the Backward-Forward sweep power flow algorithm is mainly used for distribution networks for fast and accurate results [21]. Consider a radial distribution network shown in Fig. 2. Buses r & s are connected through a line having a total impedance Z_{rs} .

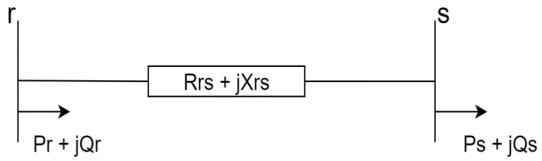

Fig. 2 Radial distribution network

$$Z_{rs} = R_{rs} + jX_{rs} \tag{8}$$

Active power loss for the line between r & s can be written as:

$$APL_{(rs)} = R_{rs}\left(\frac{P_{rs}^2 + Q_{rs}^2}{V_r^2}\right) \tag{9}$$

The total active power loss (TAPL) can be computed by:

$$TAPL = \sum_{s=1}^{N_{br}} APL_{(rs)} \tag{10}$$

where N_{br} is the total number of branches present in the network, $r = 1{:}\,N_b$ and N_b is the number of buses.

An important function of the voltage deviation (VD) is to determine the weak buses in a network. It is a measure of voltage stability margin in the power system network to maintain voltage within the permissible limits after the occurrence of disturbance. Total voltage deviation (TVD) is given by:

$$TVD = \sum_{r=1}^{N_b} |1 - V_r| \tag{11}$$

where, V_r is the voltage at bus r, $r = 1{:}\,N_b$.

In this paper, two objective functions (OF) are formulated to minimize active power loss & minimize voltage deviation index. *i.e.,* Minimize $OF1 = APF$ and Minimize $OF2 =$ TVD.

This multi-objective problem is solved using the weighted sum approach and the overall objective function (OOF) is defined in (12).

$$OOF = w_1 * TAPL + w_2 * TVD \tag{12}$$

where w_1 and w_2 are the weights of $OF1$ & $OF2$ respectively. The values considered for w_1 and w_2 are 0.7 and

0.3 respectively. The objective function in (12) is minimized with respect to the following constraints.

Power Balance Constraints

$$P_{Load}^{EVs} + P_{Load} + P_{Loss} = P_{DGs} + P_{grid} \quad (13)$$

where P_{grid}, P_{Loss} and P_{DG} are the active power of the electrical grid, active losses of the network, and power output of all DGs respectively.

$$Q_{Load} + Q_{Loss} = Q_{DGs} + Q_{grid} \quad (14)$$

where Q_{grid}, Q_{Loss} and Q_{DGs} are the reactive power of the electrical grid, reactive losses of the network, and power output of all DGs respectively.

Voltage limits of the bus

$$V_i^{min} < V_i(t) < V_i^{max} \quad i = 1,2,\ldots..N_b \quad (15)$$

where, V_i^{min} and V_i^{max} are the minimum and maximum bus voltage limits, having values 0.95 and 1.05 respectively. V_i is the voltage magnitude at bus i in pu.

Power limits of DERs

$$P_{DG,m}^{min} < P_{DG,m} < P_{DG,m}^{max} \; \forall m \in M \quad (16)$$

$$Q_{DG,m}^{min} < Q_{DG,m} < Q_{DG,m}^{max} \; \forall m \in M \quad (17)$$

where, $P_{DER,m}^{min}$ and $P_{DER,m}^{max}$ are the minimum and maximum limits on the active & reactive power output of the m^{th} DER, respectively.

A. Algorithm for capacity estimation of DG, allocation of DG and EVCS

In this paper, 3 optimization techniques are adopted to estimate the optimal capacity and placement of DG along with suitable placement of EVCS for minimizing both objective functions. The flow chart of the proposed method is shown in Fig. 3. In order to set the lower and upper limits of control parameters for optimization certain pre-assumptions are made:

- For the scenarios in which DGs are integrated into the test system, the total load of the system is fulfilled only by DGs which means that the power taken from the grid is zero. Further, the sum of capacities of all DGs present in the network is less than or equal to the total connected load on the system to restrict the over-sizing of DGs.
- DGs are permitted to be located at any bus except the grid-connected bus i.e., bus number 1.
- The total four EV charging stations are considered in this system for optimal location. Two charging stations ($RCS\ 1$ & $RCS\ 2$) are assigned to locate for residential buses. However, for a commercial and industrial group of buses, one charging station (CCS & ICS) is allocated to each group.

1) Hybrid Particle Swarm Grey Wolf Optimzation (HPSOGWO) : This algorithm is developed by Şenel, F.A., Gökçe, F., Yüksel, A.S. et al. [22]. It utilizes the GWO algorithm to support the PSO algorithm in order to reduce the possibility of falling PSO into a local minimum [23]. The flowchart of the HPSOGWO algorithm is shown in Fig. 4. The optimal results obtained from HPSOGWO are discussed in Section V.

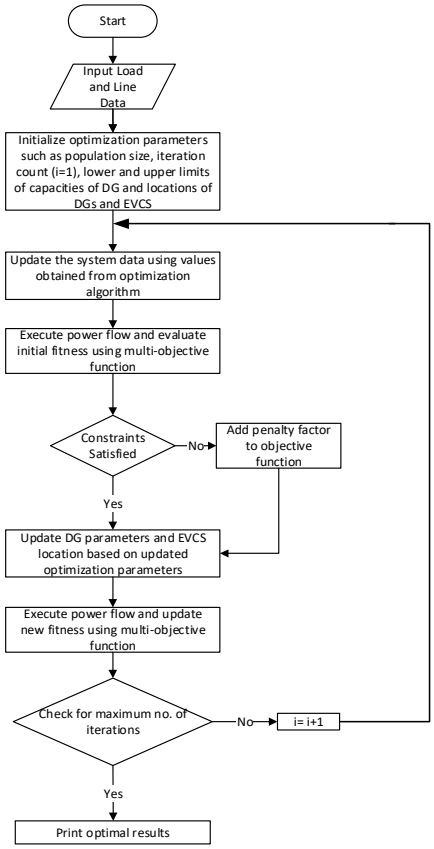

Fig. 3 Flow chart of the proposed method

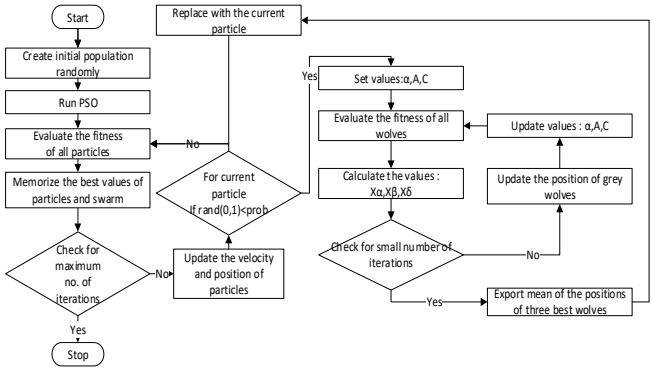

Fig. 4 Flowchart of HPSOGWO algorithm

V. CASE STUDY AND RESULTS

The IEEE 33-bus radial distribution system is considered. During the analysis, the base voltage and base MVA considered are 12.66 kV and 100 MVA respectively. The test system consists of 33 buses and 32 branches as shown in the single-line diagram depicted in Fig. 5. It is assumed that the initial total real and reactive power loads on the system (apart from EV charging load) are 3715 kW and 2300 kVAr, respectively. In this study, five scenarios are considered i.e., a test system without DG and EVCS; without DG but with EVCS; with a PV as DG and EVCS; with a PV and WTG as DG and EVCS and a test system with all the three DGs, PV, WTG, DEG, and EVCS. In scenario 2, optimum allocations of EVCS are determined using all three optimization algorithms. Moreover, for scenarios 3,4, and 5 the optimum capacity and allocations of DGs and allocations of EVCS are obtained using all three optimization algorithms. These results are summarized in Table IV.

TABLE IV. RESULTS OBTAINED FROM VARIOUS OPTIMIZATION TECHNIQUES IN ALL THE CONSIDERED SCENARIOS

Different Cases	Different Optimization Techniques	Optimal Bus No. locations of DG	Capacity of DG	Optimal EVCS Bus No. locations	Min value of TAPL (kW)	Maximum Voltage Deviation
Base Scenario 1 – Without DG and EVCS	N.A.	N.A.	N.A.	N.A.	165.7162	0.0839 at 18th bus
Scenario 2 – Without DG but with EVCS	***PSO***	N.A.	N.A.	RCS_1at 8, RCS_2at 20 CCS at 26, ICS at 24	202.22	0.0913 at 18th bus
	GWO	N.A.	N.A.	RCS_1at 8, RCS_2at 22 CCS at 26, ICS at 23	203.75	0.0913 at 18th bus
	HPSOGWO	N.A.	N.A.	RCS_1at 8, RCS_2at 19 CCS at 26, ICS at 23	201.07	0.0913 at 18th bus
Scenario 3 – With PV as DG and EVCS	***PSO***	26 (PV)	4.52 MW	RCS_1at 8, RCS_2at 21 CCS at 26, ICS at 24	123.11	0.0301 at 26th bus
	GWO	26 (PV)	4.6 MW	RCS_1at 15, RCS_2at 22 CCS at 26, ICS at 25	135.40	0.0313 at 26th bus
	HPSOGWO	26 (PV)	4.52 MW	RCS_1at 8, RCS_2at 19 CCS at 26, ICS at 23	119.7	0.03 at 26th bus
Scenario 4 – With PV and WTG as DG and EVCS	***PSO***	24 (PV) 26 (WTG)	1.6 MW (PV) 2.82 MW (WTG)	RCS_1at 8, RCS_2at 20 CCS at 29, ICS at 24	66.52	0.0377 at 18th bus
	GWO	24 (PV) 26 (WTG)	2 MW (PV) 3 MW (WTG)	RCS_1at 18, RCS_2at 22 CCS at 33, ICS at 25	90.75	0.0423 at 18th bus
	HPSOGWO	24 (PV) 26 (WTG)	1.6 MW (PV) 2.81 MW (WTG)	RCS_1at 8, RCS_2at 19 CCS at 26, ICS at 24	61.69	0.0377 at 18th bus
Scenario 5 – With PV, WTG, and DEG as DG and EVCS	***PSO***	13 (PV) 30 (WTG) 24 (DEG)	1.05 MW (PV) 1.57 MW (WTG) 1.8 MW(DEG)	RCS_1at 13, RCS_2at 22 CCS at 30, ICS at 23	32.45	0.0125 at 13th bus
	GWO	33 (PV) 13 (WTG) 24 (DEG)	1.5 MW (PV) 1.2 MW (WTG) 1.8 MW(DEG)	RCS_1at 18, RCS_2at 22 CCS at 33, ICS at 25	47.93	0.0238 at 33rd bus
	HPSOGWO	30 (PV) 11(WTG) 24 (DEG)	1.43 MW (PV) 1.2 MW (WTG) 1.8 MW(DEG)	RCS_1at 11, RCS_2at 19 CCS at 30, ICS at 24	27.98	0.0111 at 11th bus

All three optimization algorithms are iterated for 200 iterations with 70 population sizes for every scenario. Further, Fig.6, 7 and 8 shows the convergence characteristics for scenario 3, 4 and 5 respectively considering all the three optimization algorithms. In base scenario 1, the value of TAPL is lower than scenario 2 as in this case EV charging load is also considered. As observed in Table IV, for scenarios in which DG gets integrated into the test system, HPSOGWO is providing an optimal solution with the lowest TAPL and voltage deviation as compared to PSO and GWO. In scenario 3, the optimal location and capacity of DG are 26th bus and 4.52 MW respectively. It indicates that in this case approximately 904 PV arrays are required to fulfill the total load demand. The value of TAPL and maximum VD observed at these optimal solutions is 119.7 kW and 0.03 on the 26th bus respectively.

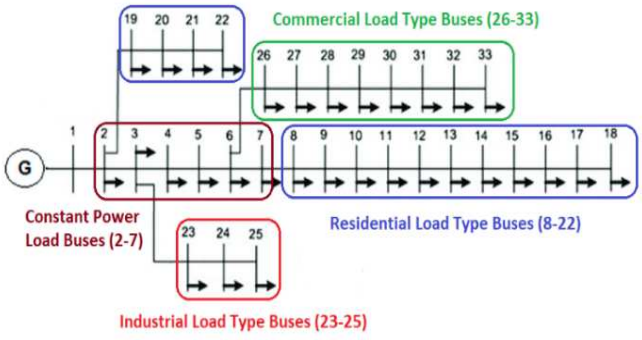

Fig. 5. IEEE 33 bus modified test system

Similarly, in scenario 4, 1.6MW rated PV allocated on the 24rd bus and 2.81 MW rated WTG on the 26th bus are the optimal solutions obtained by HPSOGWO. It means, 320 PV arrays and 19 WTGs are required in this scenario. The TAPL and maximum VD values observed in this case are 61.69 kW and 0.0377 on the 18th bus respectively. However, in scenario 5 the optimal locations and rated capacities of PV, WTG, and DEG are 30th bus with 1.43MW, 11th bus with 1.2MW, 24th bus with 1.8MW respectively. This implies that the test system requires approximately 286 PV arrays, 8 WTGs and a diesel generator of 1800kW to fulfill the total load demand. The TAPL and maximum VD value in this scenario come out to be lowest among all scenarios i.e., 27.98 kW and 0.0111 on the 11th bus. It is evident that as the number of DGs is increasing in the test system the value of TAPL is decreasing. Fig.9 shows the voltage profile in all the scenarios. It is significant from Fig.9 that the most stable voltage profile is observed for Scenerio 5 with minmum voltage deviation at each bus.

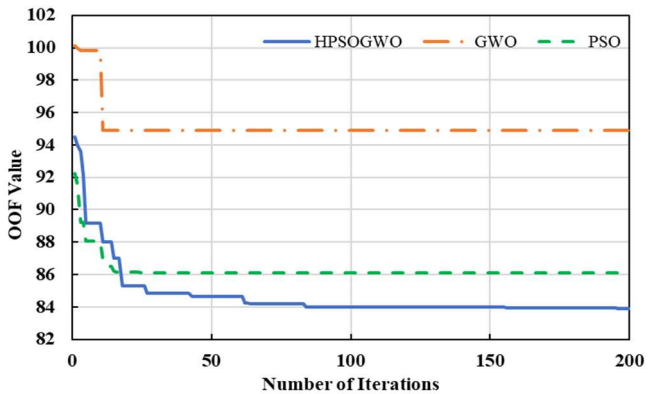

Fig. 6 Convergence characteristics for Scenario 3 considering HPSOGWO, GWO, and PSO.

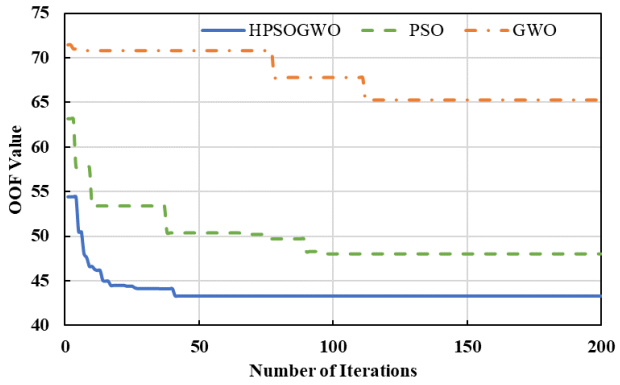

Fig. 7 Convergence characteristics for Scenario 4 considering HPSOGWO, GWO, and PSO.

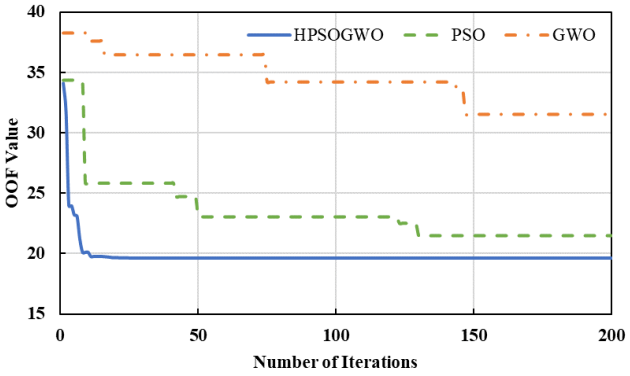

Fig. 8 Convergence characteristics for Scenario 5 considering HPSOGWO, GWO, and PSO.

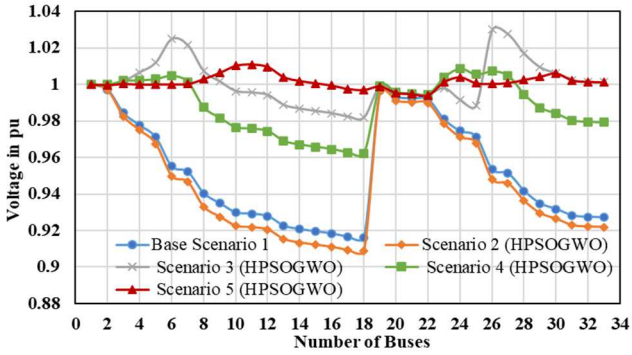

Fig. 9 Voltage profile of buses for all scenarios

VI. Conclusion

This paper proposed a method to estimate the optimal capacity and placement of multiple DGs along with EVCS optimal allocation in a practical distribution system by using various meta-heuristics optimization algorithms. The multi-objective function is employed to lower the power losses and improve voltage stability. The proposed method is tested on a modified IEEE 33 bus network having DGs based on solar photovoltaic (PV), wind turbine (WTG), and diesel generator (DEG) with voltage-dependent load models such as residential, commercial, and industrial load types. In this study, various electric vehicle charging load patterns are formulated using Monte Carlo simulations. Further, the optimal allocation of three types of Electric vehicle charging stations (EVCS), namely, Residential Charging Station (RCS), Industrial Charging Station (ICS), and Commercial Charging Station (CCS) is determined. The results show that HPSOGWO outperforms all the other algorithms for all the considered scenarios. It is also noticeable from the results that as the number of DGs is increasing in the test system the total power loss is decreasing and voltage profile is improved.

Acknowledgment

This work is supported by the Department of Science and Technology, Govt. of India, New Delhi under the “Internet of things (IoT) Research of Interdisciplinary Cyber-Physical Systems Programme” with a sanction letter DST/ICPS/CLUSTER/IoT/2018/ GENERAL.

References

[1] P. Prakash and D. K. Khatod, “Optimal sizing and siting techniques for distributed generation in distribution systems: A review,” *Renewable and Sustainable Energy Reviews*, vol. 57. Elsevier Ltd, pp. 111–130, May 01, 2016, doi: 10.1016/j.rser.2015.12.099.

[2] O. Hafez and K. Bhattacharya, “Optimal design of electric vehicle charging stations considering various energy resources,” *Renew. Energy*, vol. 107, pp. 576–589, 2017, doi: https://doi.org/10.1016/j.renene.2017.01.066.

[3] I. Diahovchenko, M. Kolcun, Z. Čonka, V. Savkiv, and R. Mykhailyshyn, “Progress and Challenges in Smart Grids: Distributed Generation, Smart Metering, Energy Storage and Smart Loads,” *Iran. J. Sci. Technol. - Trans. Electr. Eng.*, vol. 44, no. 4, pp. 1319–1333, 2020, doi: 10.1007/s40998-020-00322-8.

[4] N. Acharya, P. Mahat, and N. Mithulananthan, “An analytical approach for DG allocation in primary distribution network,” *Int. J. Electr. Power Energy Syst.*, vol. 28, no. 10, pp. 669–678, 2006, doi: 10.1016/j.ijepes.2006.02.013.

[5] R. Palanisamy and S. K. Muthusamy, “Optimal Siting and Sizing of Multiple Distributed Generation Units in Radial Distribution System Using Ant Lion Optimization Algorithm,” *J. Electr. Eng. Technol.*, vol. 16, no. 1, pp. 79–89, 2021, doi: 10.1007/s42835-020-00569-5.

[6] A. Ali, A. Youssef, T. George, and S. Kamel, “Optimal DG allocation in distribution systems using Ant lion optimizer,” *2018 Int. Conf. Innov. Trends Comput. Eng.*, pp. 324–331, 2018.

[7] M. A. Tolba, V. N. Tulsky, and A. A. Zaki Diab, “Optimal allocation and sizing of multiple distributed generators in distribution networks using a novel hybrid particle swarm optimization algorithm,” in *2017 IEEE Conference of Russian Young Researchers in Electrical and Electronic Engineering (EIConRus)*, 2017, pp. 1606–1612, doi: 10.1109/EIConRus.2017.7910880.

[8] H. Abdel-mawgoud, S. Kamel, M. Ebeed, and M. M. Aly, “An efficient hybrid approach for optimal allocation of DG in radial distribution networks,” in *2018 International Conference on Innovative Trends in Computer Engineering (ITCE)*, 2018, pp. 311–316, doi: 10.1109/ITCE.2018.8316643.

[9] J. Qiu, Z. Xu, Y. Zheng, D. Wang, and Z. Y. Dong, “Distributed generation and energy storage system planning for a distribution system operator,” *IET Renew. Power Gener.*, vol. 12, no. 12, pp. 1345–1353, 2018.

[10] R. Sanjay, T. Jayabarathi, T. Raghunathan, V. Ramesh, and N. Mithulananthan, “Optimal allocation of distributed generation using hybrid grey wolf optimizer,” *Ieee Access*, vol. 5, pp. 14807–14818, 2017.

[11] K. S. Rani, B. K. Saw, P. Achargee, and A. K. Bohre, “Optimal Sizing and Placement of Renewable DGs using GOA Considering Seasonal Variation of Load and DGs,” in *2020 International Conference on Computational Intelligence for Smart Power System and Sustainable Energy (CISPSSE)*, 2020, pp. 1–6.

[12] M. Moradijoz, M. Parsa Moghaddam, M. R. Haghifam, and E. Alishahi, “A multi-objective optimization problem for allocating parking lots in a distribution network,” *Int. J. Electr. Power Energy Syst.*, vol. 46, pp. 115–122, 2013, doi: https://doi.org/10.1016/j.ijepes.2012.10.041.

[13] M. R. Mozafar, M. H. Moradi, and M. H. Amini, “A simultaneous approach for optimal allocation of renewable energy sources and electric vehicle charging stations in smart grids based on improved GA-PSO algorithm,” *Sustain. Cities Soc.*, vol. 32, pp. 627–637, 2017, doi: https://doi.org/10.1016/j.scs.2017.05.007.

[14] S. M. Moghaddas-Tafreshi and E. Mashhour, “Distributed generation modeling for power flow studies and a three-phase unbalanced power flow solution for radial distribution systems considering distributed

generation," *Electr. Power Syst. Res.*, vol. 79, no. 4, pp. 680–686, 2009, doi: 10.1016/j.epsr.2008.10.003.

[15] H. R. Baghaee, M. Mirsalim, G. B. Gharehpetian, and H. A. Talebi, "Reliability/cost-based multi-objective Pareto optimal design of stand-alone wind/PV/FC generation microgrid system," *Energy*, vol. 115, no. October 2017, pp. 1022–1041, 2016, doi: 10.1016/j.energy.2016.09.007.

[16] "124-an-bonus-150-30 @ en.wind-turbine-models.com." [Online]. Available: https://en.wind-turbine-models.com/turbines/124-an-bonus-150-30.

[17] K. Qian, C. Zhou, M. Allan, and Y. Yuan, "Effect of load models on assessment of energy losses in distributed generation planning," *Int. J. Electr. Power Energy Syst.*, vol. 33, no. 6, pp. 1243–1250, 2011, doi: 10.1016/j.ijepes.2011.04.003.

[18] N. Rostami and M. O. Sadegh, "The Effect of Load Modeling on Load Flow Results in Distribution Systems," vol. 6, no. 1, pp. 16–27, 2018, doi: 10.12691/ajeee-6-1-3.

[19] T. Rawat and K. R. Niazi, "Impact of EV charging/discharging strategies on the optimal operation of islanded microgrid," *J. Eng.*, vol. 2019, no. 18, pp. 4819–4823, 2019, doi: 10.1049/joe.2018.9335.

[20] H. Liu, Y. Ji, H. Zhuang, and H. Wu, "Multi-objective dynamic economic dispatch of microgrid systems including vehicle-to-grid," *Energies*, vol. 8, no. 5, pp. 4476–4495, 2015, doi: 10.3390/en8054476.

[21] U. Eminoglu and M. H. Hocaoglu, "Distribution systems forward/backward sweep-based power flow algorithms: A review and comparison study," *Electr. Power Components Syst.*, vol. 37, no. 1, pp. 91–110, 2009, doi: 10.1080/15325000802322046.

[22] F. A. Şenel, F. Gökçe, A. S. Yüksel, and T. Yiğit, "A novel hybrid PSO–GWO algorithm for optimization problems," *Eng. Comput.*, vol. 35, no. 4, pp. 1359–1373, 2019, doi: 10.1007/s00366-018-0668-5.

[23] A. K. Mishra, P. Mishra, and H. D. Mathur, "Load Frequency Control of a Nonlinear Power System via Demand Response Control Strategy Based Fractional Order Fuzzy Controller," in *2020 21st National Power Systems Conference (NPSC)*, 2020, pp. 1–6, doi: 10.1109/NPSC49263.2020.9331919.